TISSUE ENGINEERING: Part A
Volume 25, Numbers 7 and 8, 2019

DOI: 10.1089/ten.tea.2018.0163

termis
Tissue Engineering
& Regenerative Medicine
International Society

ORIGINAL ARTICLE

The Effects of Metabolic Substrate Availability on Human Adipose-Derived Stem Cell Spheroid Survival

Robert Coyle, BS,[1,*] Jenny Yao,[2,*] Dylan Richards, PhD,[1] and Ying Mei, PhD[1,3]

Human adipose-derived stem cells (hADSCs) spheroids have displayed remarkable potential for treating ischemic injury. However, low nutrient (i.e., glucose and oxygen) availability in ischemic environments results in limited tissue viability posttransplantation. To develop a mechanistic understanding of nutrient levels on spheroid survival, we used an *in vitro* culture system to investigate the effects of varying glucose and oxygen concentrations on the cellular viability of hADSC spheroids with varied radii (115–215 μm). Our data showed that low viability can be improved with higher levels of glucose, but not with enhanced availability of oxygen. To understand the experimental results, we established a computational model to simulate nutrient diffusion and metabolism in hADSC spheroids at different glucose and oxygen concentrations. By combining experimental data and modeling results, we established a strong linear correlation ($R^2 = 0.84$) between spheroid glucose availability (i.e., spheroid volume with available glucose) and spheroid viability. In contrast, increasing oxygen availability had negligible impact on spheroid viability, suggesting a greater dependence on anaerobic glycolysis for adenosine triphosphate generation as opposed to oxidative phosphorylation. These data demonstrated the critical role of glucose in hADSC spheroid survival under ischemia. These results may impact future strategies for improving hADSC transplantation efficacy through codelivery of metabolic substrates.

Keywords: adipose-derived stem cell, spheroid, ischemia, nutrient diffusion, mathematical modeling, 3D tissue culture

Impact Statement

Human adipose-derived stem cells (hADSCs) spheroids have displayed remarkable potential for treating ischemic injury. However, low nutrient (i.e., glucose and oxygen) availability in ischemic environments results in limited tissue viability posttransplantation. To develop an understanding of the effects of nutrient availability on spheroid survival, we utilized both *in vitro* and computational models to examine the limiting factors in metabolic supply for avascular microtissues, revealing the critical role of glucose to improve hADSC spheroid survival in ischemic conditions. These results may impact future strategies for improving hADSC transplantation efficacy through codelivery of metabolic substrates.

Introduction

Human adipose-derived stem cells (hADSCs) possess great therapeutic promise in treating ischemic diseases.[1–8] To this end, Kaneda *et al.* reported the improvement of endothelial cell viability and recruitment after hADSC injections at hindlimb ischemic injury sites through the secretion of vascular endothelial growth factor and hepatocyte growth factor.[9] However, low cellular retention and survival posttransplantation have limited their translational potential.[10–12] Previous studies have shown that a majority of cells (~95–99%) are lost within the first 72 h following transplantation, a phenomenon attributable to anoikis-mediated cell death, hypoxia-induced apoptosis, nutrient starvation, and so on.[13–16] To address this challenge, tissue-engineered constructs have been developed to improve cell retention and viability following transplantation.[17,18] The advantages of tissue-engineered constructs include enhanced cell–cell communication, preserved extracellular matrix signaling, and an upregulation of paracrine factor secretion.[19] For example,

[1]Department of Bioengineering, Clemson University, Charleston, South Carolina.
[2]Academic Magnet High School, North Charleston, South Carolina.
[3]Department of Regenerative Medicine and Cell Biology, Medical University of South Carolina, Charleston, South Carolina.
*These authors have equally contributed to this work.

Lin *et al.* have applied hADSC sheet technology to treat an acute myocardial infarction rat model.[20] Their results showed improved cardiac function, cytokine expression, and long-term hADSC engraftment compared to intramyocardial injection of dissociated hADSCs.

hADSC spheroids have recently received increasing attention due to their spherical microtissue configuration, which predisposes them to conventional catheter-based delivery technologies.[21,22] However, the avascular nature of these microtissues presents its own challenges due to a greater reliance on nutrient diffusion, creating an upper limit on tissue size/thickness.[23] Although this limitation may not cause noticeable strain under controlled culturing conditions, transplantation into an ischemic environment may result in significant cell death because of the decreased availability of metabolic substrates (i.e., glucose and oxygen).[24,25] While it is well established that nutrient supply in the ischemic environment plays a significant role in tissue viability posttransplantation,[15,26–28] it is not yet clear as which nutrient (i.e., glucose or oxygen) plays a more significant role in maintaining hADSC viability posttransplantation.[29] Although glycolysis is the primary source of adenosine triphosphate (ATP) production in hADSC culture, oxygen enables the more efficient consumption of glucose via aerobic metabolism, perhaps necessary to meet increased metabolic demands of cells in dense microtissue constructs.[29–31] Thus, this study aimed to examine the effects of nutrient availability on hADSC spheroid viability as to accelerate their clinical translation. Notably, the spherical shape of spheroid microtissues provides an ideal system to experimentally determine and mathematically model nutrient diffusion and consumption. In this study, we demonstrate that availability of glucose, instead of oxygen, is the limiting factor in determining cell viability for hADSC spheroids under ischemic conditions. These results provide important insight toward development of future hADSC-based tissue engineering constructs to treat ischemic diseases.

Materials and Methods

hADSC spheroid fabrication

The hADSCs (Lonza, Basel, Switzerland) were cultured according to the manufacturer's protocol. hADSCs were seeded on 0.1% gelatin-coated T-75 flasks with plating growth media (Bulletkit ADSC, Lonza) at a seeding density of 0.75 million cells per flask and incubated at 37°C/5% CO_2 for 3 days. Cells in passage 6–7 were used in the experiments. The agarose hydrogel molds used were prepared using commercial master micro molds from Microtissues, Inc (Providence, RI) as negative replicates to create nonadhesive agarose hydrogel molds. Each agarose mold contains 35 concave recesses with hemispheric bottoms (800 μm diameter, 800 μm depth) to facilitate the formation of hADSC spheroids. In brief, 330 μL of 2% sterile agarose solution was pipetted onto the master micro molds, and the newly formed agarose molds were carefully detached from the master mold after gelation and transferred into a 35/10 mm polystyrene Petri dish. Approximately 80 μL of the hADSC suspension was then pipetted into each agarose mold, resulting in the formation of 35 similarly sized hADSC spheroids. To achieve spheroids of varying sizes, we used cell solutions of varying concentrations during the seeding step. To achieve spheroids with radii of 115, 135, 175, and 215 μm, we used cell solutions of 0.5, 1.0, 2.5, and 5.0 million cells/mL, respectively. Adapted from Ref.[32]

In vitro *ischemic treatment*

Ischemic conditions were simulated *in vitro* through a combination of hypoxic culture conditions and ischemic media. Hypoxic conditions were produced through the use of a hypoxia chamber (ProOx Model 110; BioSpherix, Parish, NY) set to 1% O_2. Ischemic media was produced through the dilution of hADSC maintenance media (High-Glucose DMEM, Gibco Life Technologies, Grand Island, NY supplemented with 15% fetal bovine serum and 1% penicillin–streptomycin) with nine times the amount of glucose-free/serum-free medium (Glucose-Free DMEM, Gibco) (v/v). hADSC spheroids were cultured for up to 72 h in conditions defined as Control (maintenance media with 5.5 mM glucose, 21% O_2), Ischemic (ischemic media with 0.55 mM glucose, 1% O_2), Ischemic + Glucose (ischemic media with added glucose but without other components resulting in a glucose concentration of 5.5 mM, 1% O_2), and Ischemic + Oxygen (ischemic media with 0.55 mM glucose, 21% O_2). 2,4-dinitrophenol (DNP) treatment adapted from Ref.[33] In brief, we added 2 μM concentrations of the mitochondrial uncoupler DNP to the maintenance media 24 h before treatment conditions for hADSC spheroids measuring a radius of 135 μm to inhibit oxidative phosphorylation. We then exposed the hADSC spheroids to each of the treatment conditions +2 μM DNP for 72 h.

TUNEL assay and viability assessment

Roche *In Situ* Cell Death Detection Kit (Sigma-Aldrich, St. Louis, MO) was used to visualize cell viability in frozen sections of hADSC spheroids based on the Roche protocol. In brief, hADSC spheroid frozen sections were fixed with 4% paraformaldehyde in phosphate buffered saline (PBS) for 20 min at room temperature. After washing in PBS for 30 min, samples were incubated in a permeabilization solution (0.1% Triton X-100 and 0.1% sodium citrate in PBS) for 2 min on ice. Then, 50 μL of the TUNEL reaction mixture was added to samples and incubated at 37°C for 1 h. After washing in PBS (2 times, 5 min), nuclei were counterstained with 4′,6-diamidino-2-phenylindole (DAPI) (Molecular Probes/Invitrogen) diluted in PBS for 15 min at ambient temperature. Following the final wash procedure (PBS, 2 times, 5 min), glass cover slips were placed on the slides using Fluoro-Gel (Electron Microscopy Sciences). A TCS SP5 AOBS laser scanning confocal microscope (Leica Microsystems) was used for imaging. Quantification of viability was achieved using ImageJ particle analysis. In brief, we quantified the overall number of nuclei represented per spheroid through DAPI staining, followed by a quantification of the total number of TUNEL-positive nuclei for the corresponding spheroid. We then used the complementary percentage of the ratio between TUNEL-positive nuclei to total nuclei to estimate the percentage of viable hADSCs per spheroid cross-section in defining the ''Viability Index'' for each spheroid size and culture condition. To study the effect of culture conditions on cell viability, the change in viability (Δ% Viability Index) in each culture condition compared with the ischemic condition was calculated for each spheroid size group. For each culturing condition and time point during the 72 h, we quantified at least $n = 8$ spheroids.

Lactate concentration measurements

Media samples (100 μL) were collected from 115 and 175 μm spheroid size groups for each culture condition (+Oxy/+Glu, −Oxy/+Glu, +Oxy/−Glu, and −Oxy/−Glu) at 3, 6, 24, 48, and 72 h time points. Samples from media were measured in triplicate with the YSI 2700 Select Biochemistry Analyzer (YSI, Inc., Yellow Springs, OH).

Defining computational model

A computational model coupling energy metabolism and nutrient diffusion was developed to predict glucose, oxygen, lactate, and ATP profiles within the hADSC spheroids. A finite element model of oxygen, glucose, and lactate transport within hADSC spheroids was developed based on Fick's Second Law of Diffusion.[34] In a spherical coordinate system, the oxygen, glucose, and lactate concentration profiles are governed by the equation:

$$\frac{D}{r^2}\frac{\partial}{\partial r}\left(r^2\frac{\partial C}{\partial r}\right) - R = 0,$$

where C represents nutrient concentration, r radial distance from spheroid center, D nutrient diffusivity, and R nutrient consumption (oxygen and glucose) or metabolite production (lactate) rate. For this study, diffusivity values of:

$$D_{Ox} = 3.0\times10^{-6}\text{cm}^2/\text{s}$$

$$D_{Gluc} = 3.9\times10^{-7}\text{cm}^2/\text{s}$$

$$D_{Lac} = 4.68\times10^{-7}\text{cm}^2/\text{s},$$

derived from Brown *et al.* and Rumsey *et al.*[25,35] Next, hADSC concentration-dependent nutrient consumption rates were modeled by the Michaelis–Menten equation:

$$R = \rho_c\frac{V_{\max}[\text{C}]}{K_m + [\text{C}]},$$

where ρ_c represents spheroid cell density, V_{max} maximum rate at high substrate concentration, and K_m Michaelis–Menten constant.

The consumption rate constants for oxygen were derived from a study by Brown *et al.* (25, 30):

$$V_{max} = 5.44\times10^{-8}\text{ nmol/cell/s}$$

$$K_m = 3.79\text{ nmol/mL}$$

The consumption rate constants for glucose were derived from a study by Mischen *et al.* (25, 29):

$$V_{max} = 2.31\times10^{-7}\text{ nmol/cell/s}$$

$$K_m = 40.0\text{ nmol/mL}$$

To simulate the coupled metabolic rates (oxygen consumption, glucose consumption, and lactate production) in primary energy metabolism, cellular respiration and energy production equations from a study by Venkatasubramanian *et al.*[36] were adapted for the model (Supplementary Fig. S1; Supplementary Data are available online at www.liebertpub.com/tea). For the purposes of this experiment, we assumed ATP production as described in Supplementary Figure S2.

Analysis of computational model

The control and ischemic culture conditions established in the experimental viability assays were accounted for in the boundary conditions of the finite element model. Once all the equations were compiled, the finite element model was numerically solved by the software COMSOL Multiphysics (COMSOL, Inc., Burlington, MA), from which the oxygen, glucose, and lactate concentration profiles were determined in spheroids of radii 115, 135, 175, and 215 μm. Considering the axial symmetry of spheroids, the hemispherical concentration profiles obtained by solving the model on COMSOL were plotted into line graphs that showed the change in nutrient/metabolite concentration based on radial position from the spheroid center. The nutrient consumption rates with respect to distance from the spheroid center (Fig. 3C–F) were then used to determine a lower threshold for a functional nutrient consumption rate (glucose/oxygen) to quantify the nutrient availability across spheroid groups and culture conditions. The nutrient availability in a spheroid was defined as a complementary percentage of the ratio between spheroid volume with the nutrient (above the threshold consumption rate) to the total spheroid volume. To study the effect of culture conditions on nutrient availability, the change in nutrient availability (Δ% Glucose/Oxygen availability) in each culture condition compared with the ischemic condition was calculated for each spheroid size group. To quantify the relationship between cell survival and nutrient availability of oxygen and glucose, the change in viability index values (Δ% Viability Index) and the change in nutrient availability (Δ% Glucose/Oxygen Availability) were plotted to determine if they exhibited a correlational relationship.

Statistical methods

Differences between experimental groups were analyzed on JMP Pro 12 Statistical software (SAS, Cary, NC) using Student's *t*-test, matched pairs comparison, one-way ANOVA, and two-way ANOVA with Tukey's *post hoc* test, and $p<0.05$ was considered significantly different for all statistical tests.

Results

hADSC spheroids as model for nutrient diffusion through avascular tissue

Spheroids provide an enabling platform for delivering hADSCs to areas of ischemic injury. However, the low availability of metabolic substrates in these ischemic sites can significantly limit cell survival due to inadequate nutrient diffusion. To investigate the effects of metabolic substrate availability on cell viability, we developed a robust fabrication technique to consistently produce spheroids of varying radii (115, 135, 175, and 215 μm) (Fig. 1A, B). With

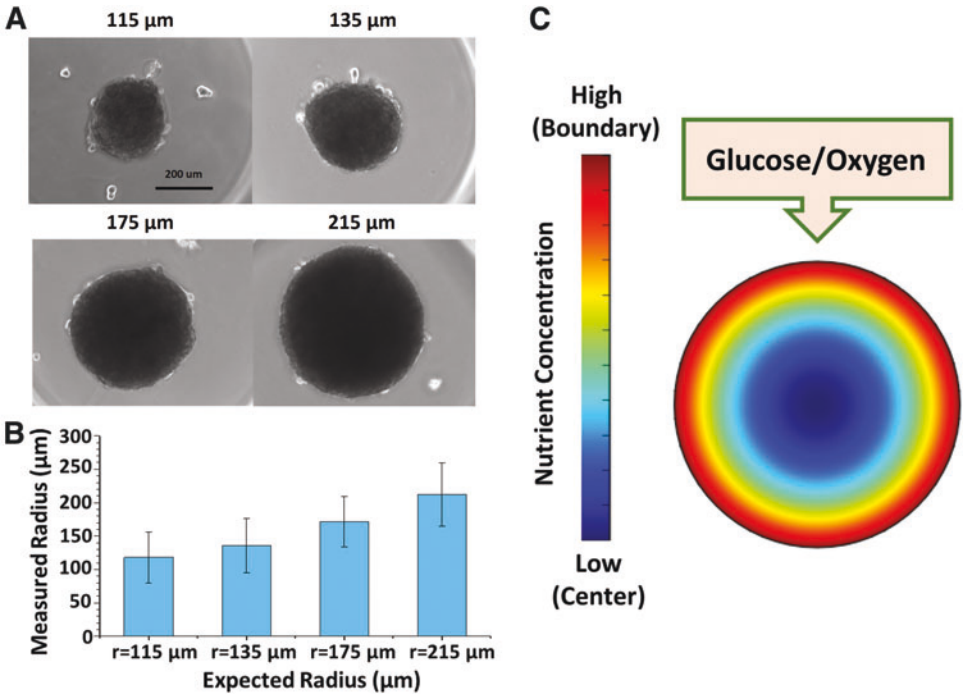

FIG. 1. hADSC spheroids provide an ideal model to test the effects of nutrient availability on viability. **(A)** Representative images of hADSC spheroids of four radii (115, 135, 175, and 215 µm). **(B)** Fabrication techniques produced hADSC spheroids of consistent and significantly different size (x-axis nominal radii, y-axis measured radii). **(C)** General nutrient consumption surface plot representing how nutrient (i.e., glucose/oxygen) concentrations decrease contiguously from the spheroid surface to the center. Low nutrient levels at the center may not be sufficient to meet hADSC metabolic demands and result in an apoptotic core. Color images are available online.

the reported diffusion limits for oxygen through dense, avascular tissue being ~100–200 µm,[37,38] the sizes selected here can represent a wide range of nutrient availability within the spheroids (Fig. 1C).

Nutrient diffusion as limiting factor in cellular viability of hADSC spheroid

To investigate metabolic strain on viability, we established an *in vitro* tissue culture model to simulate the ischemic environment. These conditions were defined by two characteristics: (1) low availability of carbon substrate, simulated with 10% of normal glucose concentration (0.55 mM), and (2) low availability of oxygen, simulated with a hypoxia environment (1% O_2).[16,29] Spheroids were exposed to ischemic conditions for 72 h, as this range of time corresponds with the majority of all transplanted cell death and serves as a critical window for understanding cell survival posttransplantation.[13–16] For the purposes of this study, we were primarily interested in the role that metabolite diffusion and availability plays in governing cell survival of hADSC spheroids under ischemic strain. As such, TUNEL staining was used to assess the viability of spheroid cells after exposure to testing conditions. (Fig. 2A) After 72 h, spheroids cultured under control conditions (21% oxygen, 5.5 mM glucose, +Oxy/+Glu) showed a general decrease in viability with respect to increasing diameter. (Fig. 2B) However, spheroids cultured under ischemic conditions (1% oxygen, 0.55 mM glucose, –Oxy/–Glu) exhibited a similar yet more severe pattern of declining cell viability with respect to increasing spheroid diameter (Fig. 2B). When comparing spheroids in the control condition with the ischemic ones, there exists a reduction of cellular viability of 8% for 115 µm, 26% for 135 µm, 25% for 175 µm, and 40% for 215 µm spheroids (Supplementary Fig. S3A). These data strongly support that low nutrient availability for the cells at the spheroid center plays a critical role in decreased cellular viability.

To more closely investigate the individual effects of glucose availability and oxygen availability on spheroid viability, we reintroduced the two primary nutrients (i.e., oxygen and glucose) to our ischemic model, resulting in ischemia + oxygen (+Oxy/–Glu) and ischemia + glucose (–Oxy/+Glu) conditions (Fig 2B). Reintroducing oxygen (21%) while maintaining low glucose (0.55 mM) (+Oxy/–Glu) resulted in varying degrees of increased viability over ischemic spheroids. Yet, conversely, reintroducing glucose (5.5 mM glucose) while maintaining low oxygen (1%) (–Oxy/+Glu) yielded a significant improvement in cellular viability over ischemia (Supplementary Fig. S3B). The increased viability is particularly evident for the larger spheroids (215 µm), with –Oxy/+Glu producing a much higher viability than +Oxy/–Glu or Ischemia. These results strongly suggest that glucose availability contributes to hADSC spheroid survival significantly more than oxygen availability.

Mathematical modeling of nutrient diffusion and consumption in hADSC spheroids

To develop a fundamental understanding of metabolic substrate diffusion and metabolism in hADSC spheroids, we adapted existing models simulating nutrient diffusion and consumption through microtissues and established a finite element computational model to quantify the relationship among spheroid diameter, culture condition, and nutrient availability.[25,34,36,39,40] To account for the duality of aerobic and anaerobic metabolism (i.e., shifting between glycolysis and oxidative phosphorylation for ATP synthesis due to substrate diffusivity differences and concentration-dependent consumption rates), the model incorporated a coupled relationship between oxygen and glucose uptake. Using parameters derived from literature (see Materials and Methods

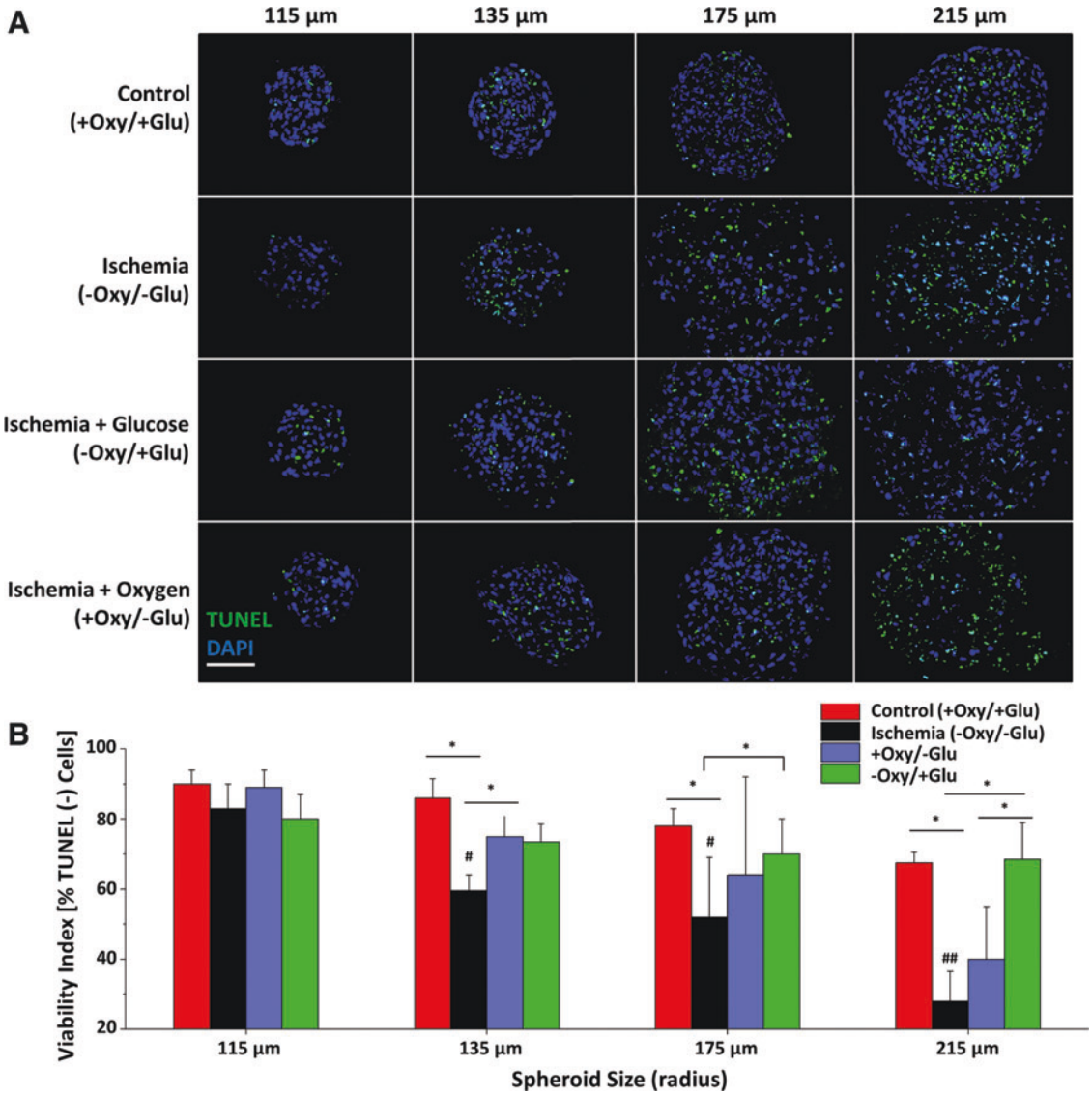

FIG. 2. hADSC viability is dependent upon spheroid size and availability of metabolic substrates. **(A)** Representative immunofluorescence images showing TUNEL staining of hADSC spheroids after 72 h of exposure to each of the defined testing conditions. Four culture conditions were chosen to assess the effects of metabolic availability on hADSC spheroids. These conditions include Control (+Oxy/+Glu, 21% oxygen; 5.5 mM glucose), Ischemia (–Oxy/–Glu, 1% oxygen; 0.55 mM glucose), Ischemia + Glucose (–Oxy/+Glu, 1% Oxygen; 5.5 mM glucose), and Ischemia + Oxygen (+Oxy/–Glu, 21% oxygen; 0.55 mM glucose). Scale bar = 100 µm. **(B)** Quantification of spheroid viability after 72 h of exposure under each condition for each size group. For each culturing condition, $n = 8$ spheroids. $^{\#,\#\#}$Significant difference between ischemic conditions across spheroids size groups ($p < 0.05$). *Significant difference between culture conditions for each spheroid size group ($p < 0.05$). Color images are available online.

section),[25,29,30,35] we plotted glucose (Fig. 3A, B) and oxygen (Supplementary Fig. S4) concentration profiles relative to radial position from the spheroid center for each of the spheroid sizes and culture conditions. The plots showed that glucose availability in the spheroids exposed to ''Low Glucose'' conditions (–Oxy/–Glu and +Oxy/–Glu) are significantly lower than those placed in ''High Glucose'' conditions (+Oxy/+Glu and –Oxy/+Glu). Notably, glucose concentration profiles were identical for +Oxy/+Glu (control) and –Oxy/+Glu, with a similar trend identified for oxygen distribution in –Oxy/+Glu and +Oxy/+Glu conditions (Supplementary Fig. S4). These data suggest that according to our model, glucose availability in the spheroids is dependent upon glucose distribution as a function of media concentration and tissue diffusivity, while being independent of oxygen availability.

To determine spheroid glucose availability (i.e., spheroid volume with available glucose), we plotted glucose consumption rates for both the High-Glucose (+Oxy/+Glu, –Oxy/+Glu) and Low-Glucose (–Oxy/–Glu, +Oxy/–Glu) condition spheroids for each size (Fig. 3C–F). In accordance with the overall trend of the Michaelis–Menten model, as glucose concentration approaches zero, there is a dramatic concentration-dependent decrease in local glucose consumption rate. Therefore, given the small range in radial position over which consumption rate falls, we defined a glucose consumption rate of 0.0048 nmol/mm^3/s (i.e., ~10% of the

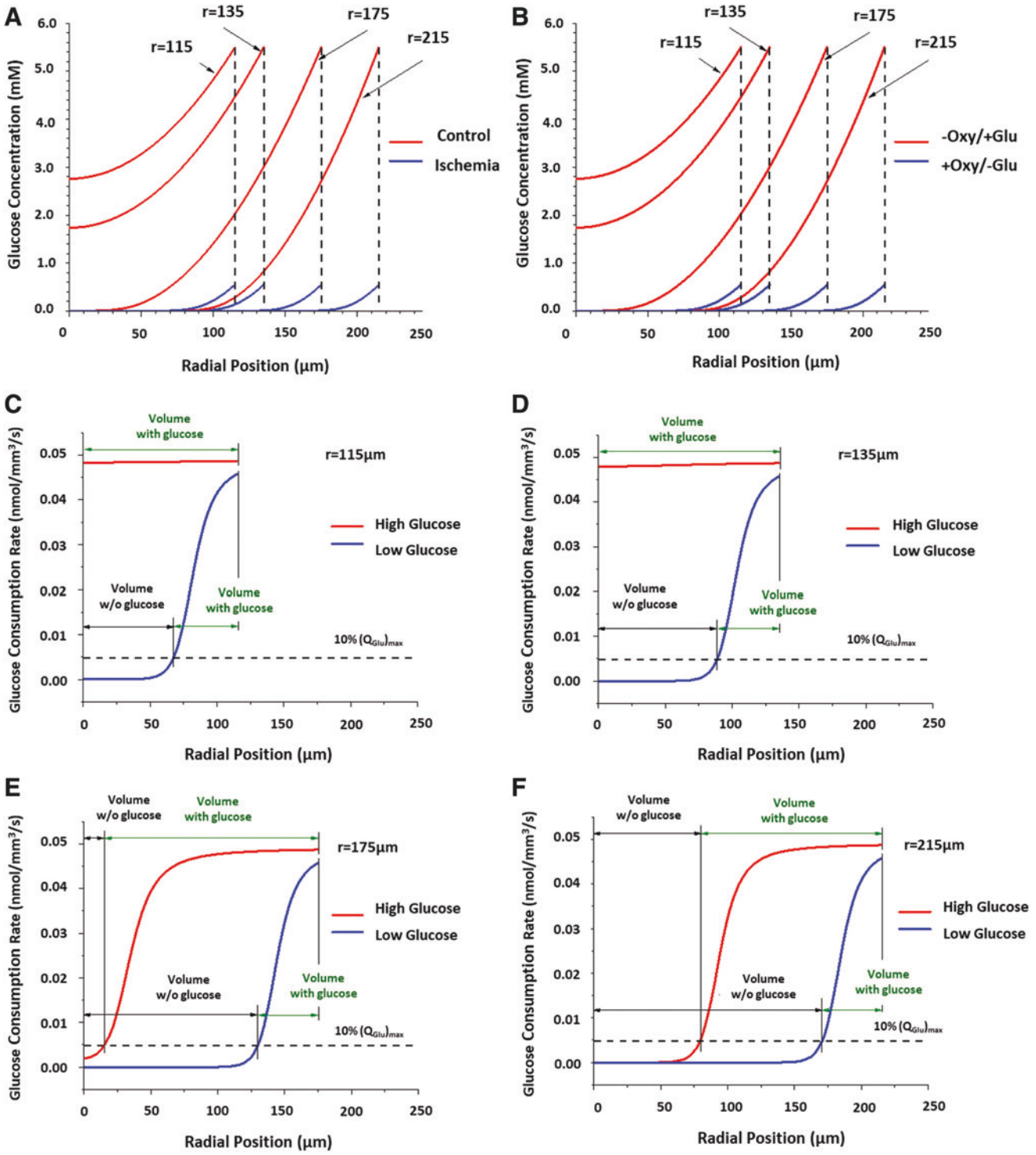

FIG. 3. Glucose concentration and consumption rates are dependent upon spheroid size and culture conditions. **(A)** Plots showing modeled glucose concentrations for different-sized spheroids under control (+Oxy/+Glu) and ischemic (−Oxy/−Glu) conditions. **(B)** Plots showing modeled glucose concentrations for different-sized spheroids under ischemic + glucose (−Oxy/+Glu) and ischemic + oxygen (+Oxy/−Glu) conditions. Glucose concentration for Control and −Oxy/+Glu are identical (same trend for Ischemia and +Oxy/−Glu). **(C–F)** Plots showing modeled glucose consumption rates under ''High Glucose'' (Control, −Oxy/+Glu) and ''Low Glucose'' (Ischemic, +Oxy/−Glu) conditions for spheroid radii of **(C)** 115 μm, **(D)** 135 μm, **(E)** 175 μm, and **(F)** 215 μm. Color images are available online.

consumption rate at the spheroid surface) as the functional glucose depletion threshold, corresponding to a glucose concentration of 0.005 mM. Delineating this value allowed us to identify the radial location of functional glucose depletion and determine spheroid glucose availability across sizes and culture conditions.

After defining the threshold for the functional depletion of available glucose, we examined the relationship between the point of functional glucose depletion with respect to spheroid volume across all spheroid sizes for both low and high glucose concentrations. As shown in Figure 4A, there is a significantly greater difference between glucose depletion locations as a function of volume for the larger spheroids compared with the smaller spheroids. For example, the smallest spheroid group (i.e., 115 μm) showed a 20% improvement in normalized spheroid volume with available glucose between low- and high-glucose culture conditions, while the largest spheroid group (i.e., 215 μm) showed an improvement of 45% in normalized spheroid volume with available glucose. To study effects of glucose availability on spheroid viability, we plotted the change in viability (Δ% Viability Index) (data derived from Supplementary Fig. S3) and change in normalized spheroid volume with available glucose (Δ% Glucose Availability) (data derived from Fig. 4A) for each spheroid size under control (+Oxy/+Glu) and ischemic + glucose (−Oxy/+Glu) conditions with respect to ischemia (−Oxy/−Glu) (Fig. 4B). The trends show that there exists a positive correlation between glucose availability and cell viability ($R^2 = 0.84$, $p < 0.001$). In contrast, when using the same methods to compare Δ% Viability Index and Δ% Glucose Availability for each spheroid group under +Oxy/−Glu conditions to those values in ischemia (−Oxy/−Glu), there did not appear to be a significant improvement in either viability or glucose availability (Supplementary Fig. S5A). In addition, there was effectively no relationship when comparing change in viability (Δ% Viability Index) and change in spheroid volume with available oxygen (Δ% Oxygen Availability) for any size group after using the same linear regression methods (Supplementary Fig. S5B).

In addition, we also investigated the rate at which lactate (lactic acid) is produced and diffuses through the hADSC spheroids, as lactate accumulation is an important byproduct of anaerobic glycolysis (Supplementary Fig. S2) and can impact hADSC metabolic activity and function.[29] We measured the lactate concentrations in media for both 115 and 175 μm size spheroid groups at each of the culture conditions over the 72-h culture period. (Fig. 5A, B) These two spheroid sizes were selected to represent smaller (115 and 135 μm) and larger (175 and 215 μm) spheroid groups, respectively. They showed significantly different viability at each of the culture conditions at 72 h (Fig. 2) and distinctly different glucose concentration profiles through modeling (Fig. 3). As shown in the Figure 5C, D, higher glucose starting conditions (+Oxy/+Glu, −Oxy/+Glu) led to higher concentrations of lactate when compared with low glucose starting conditions (−Oxy/−Glu, +Oxy/−−Glu). This suggests that a sufficient supply of glucose is essential for lactate to produce and accumulate, which is further supported by the modeling data. As a result, there is limited production of lactate under ischemic (−Oxy/−Glu) and +Oxy/−Glu conditions. Importantly, there is no determinable correlation between lactate accumulation and decreased cell viability (Supplementary Fig. S6). This demonstrates that lactate accumulation did not play a significant role in the spheroid viability in the current studies.

Computational modeling reveals dependence upon anaerobic glycolysis as primary means of ATP synthesis for hADSC spheroids

To further understand the mechanism underlying the positive linear correlation between glucose availability and cell viability, the ATP production profiles for the four nutrient

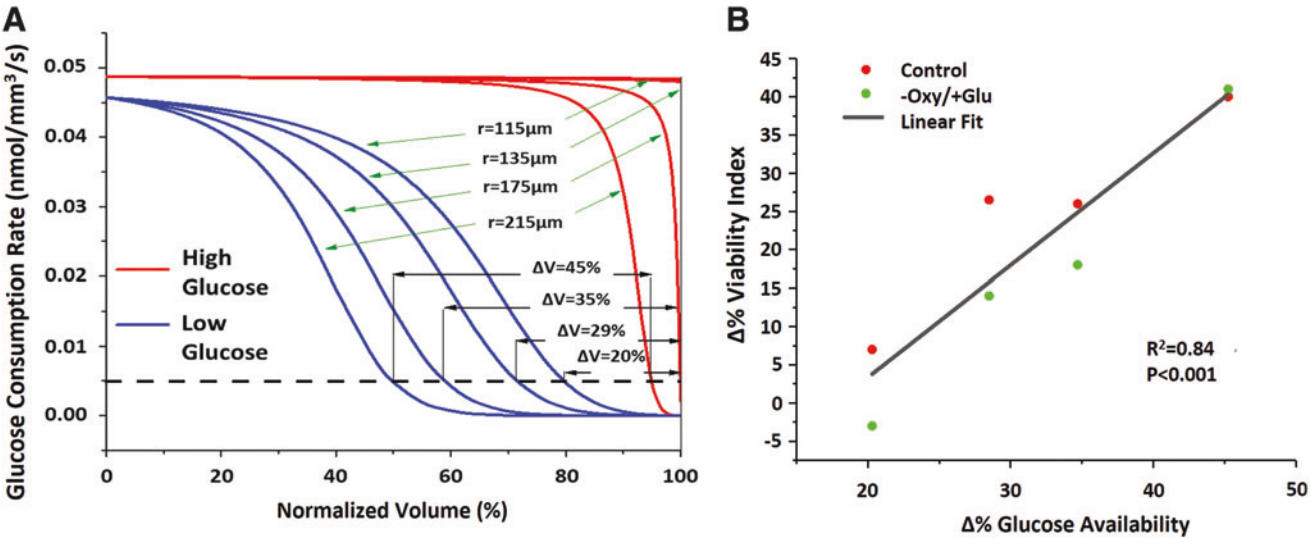

FIG. 4. Increased glucose availability positively correlates with improved hADSC viability. **(A)** Plot shows the relationship between glucose consumption rate with respect to spheroid volume at the High- and Low-glucose culture conditions. The dotted line defines the glucose consumption rate threshold, at which functional glucose consumption is depleted. **(B)** Plot illustrating that increased glucose availability positively correlates with increased spheroid viability ($p < 0.001$). Color images are available online.

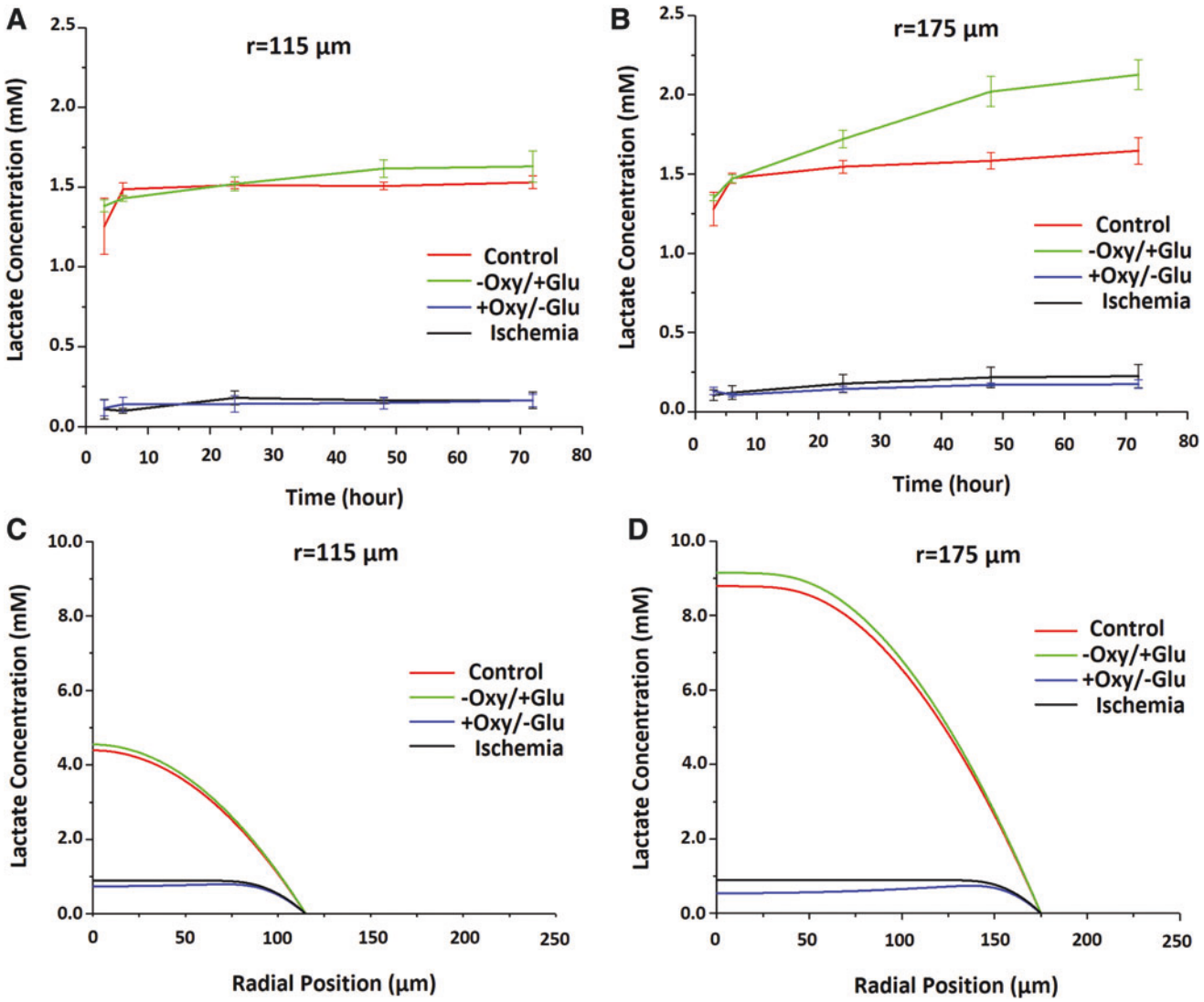

FIG. 5. Lactate concentration and accumulation is dependent upon spheroid size and culture conditions. **(A, B)** Plots showing lactate concentrations recorded periodically over a 72 h time period for spheroids of 115 µm **(A)** and 175 µm **(B)** radii under control (+Oxy/+Glu), ischemic + glucose (–Oxy/+Glu), ischemic + oxygen (+Oxy/–Glu), and ischemic (–Oxy/–Glu) culturing conditions. For each culture condition and observation period, $n = 3$. **(C, D)** Plots showing modeled lactate concentrations under control (+Oxy/+Glu), ischemic + glucose (–Oxy/+Glu), ischemic + oxygen (+Oxy/–Glu), and ischemic (–Oxy/–Glu) culturing conditions for spheroid radii of **(C)** 115 µm and **(D)** 175 µm. Color images are available online.

conditions were modeled using COMSOL to identify the primary metabolic pathway (i.e., anaerobic glycolysis or oxidative respiration) responsible for satisfying hADSC spheroid energy demands. For this study, we chose the 135 µm spheroid as our model, as it is a spheroid size that exhibits a statistical difference in viability between control and ischemic culture conditions at 72 h (Fig. 2B), and constitutes a relevant spheroid size used in previous translational studies in the literature.[21] As seen in Figure 6A, the greatest and most consistent level of total ATP production occurred under control (+Oxy/+Glu) conditions, as both nutrients are readily available to diffuse into the spheroid volume and maintain adequate metabolic activity, while the ischemic aggregates exhibited a steep decline in overall ATP synthesis beyond the surface. In comparing the individual effects of oxygen and glucose, the +Oxy/–Glu conditions resulted in a greater ATP synthesis rate at the spheroid surface, likely because, although glycolysis still dominates, the more metabolically efficient process of oxidative phosphorylation contributes more significantly to ATP production overall at the surface. Due to the rapid depletion of glucose, however, the total ATP production in +Oxy/–Glu ceased beyond the immediate surface, despite higher oxygen availability compared to ischemia. In contrast, spheroids cultured under –Oxy/+Glu showed an initially lower but overall more uniform level of ATP production throughout the spheroid volume, which suggests that glucose possesses greater influence on hADSC spheroid metabolism than oxygen.

However, to elucidate the mechanistic metabolic basis behind glucose dominance in facilitating energy production, the ratio of glycolysis-generated ATP to total ATP was plotted to distinguish relative energy contributions of

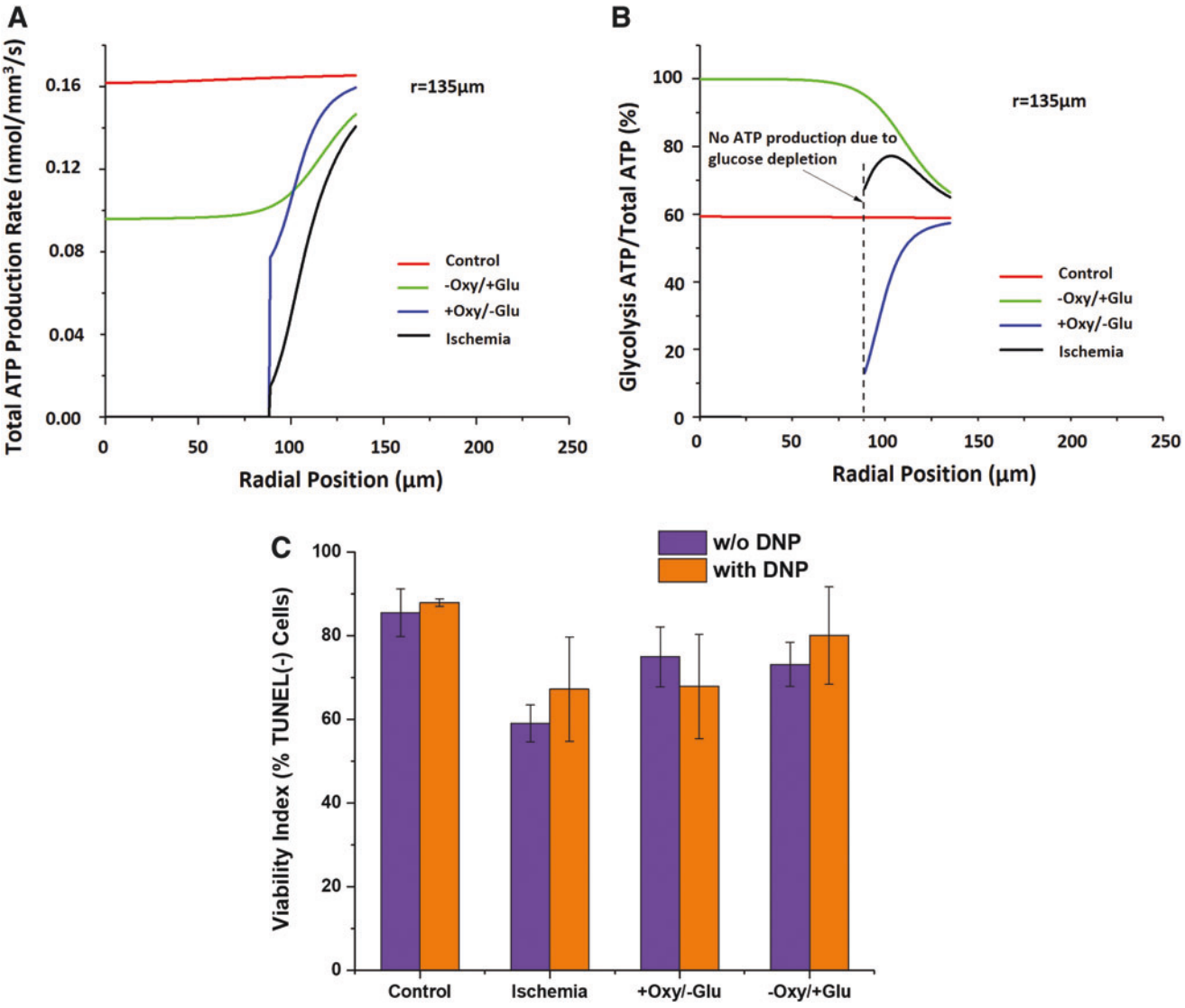

FIG. 6. Modeling ATP production in hADSC spheroids. **(A)** Total ATP production profiles for spheroids of $r = 135\,\mu m$ under four culture conditions. **(B)** Distributions of glycolytic to total ATP ratio in spheroids of $r = 135\,\mu m$ under four nutrient conditions. The curve for the ischemic and +Oxy/–Glu groups end at the radial position, at which ATP production ceased due to glucose depletion. **(C)** Investigation of preferential hADSC dependence on anaerobic glycolysis through mitochondrial inhibition on spheroid ($\sim 135\,\mu m$) viability under different culture conditions. ATP, adenosine triphosphate. Color images are available online.

anaerobic and aerobic respiration. Figure 6B demonstrates that glycolysis constitutes almost 100% of the ATP for –Oxy/+Glu spheroids. Although the +Oxy/–Glu group had the lowest ratio of glycolytic-to-total ATP synthesis, the higher energy production rate at the surface suggests that a portion of ATP was produced via oxidative phosphorylation. Interestingly, in the control group, even in the presence of ample oxygen, around 60% of the total ATP produced was derived from glycolysis, thereby implying that anaerobic respiration dominates ATP synthesis in hADSC spheroids.

To experimentally support the modeling results that glucose concentration contributes to spheroid survival significantly more than oxygen levels, we made use of the mitochondrial inhibitor DNP, which would impair spheroid ability to perform aerobic metabolism, thereby verifying the model's ATP pathway predictions. We first treated 135 μm spheroids with DNP for 72 h to allow for sufficient uptake. We then exposed the spheroids to each of the four testing conditions for an additional 72 h (Fig. 6C). The results showed that inhibiting aerobic metabolism did not significantly impact hADSC spheroid viability ($p > 0.2$), confirming that oxygen availability would not constitute a determining factor in nutrient-dependent hADSC spheroid survival posttransplantation. The data also suggest that treatment with DNP did not engender any detrimental effects to the control group.

Increased glucose availability mitigates detrimental effects of ischemic conditions on cell viability for larger spheroids with respect to time

To more thoroughly demonstrate the effect of reintroducing glucose to ischemic conditions on spheroid viability as

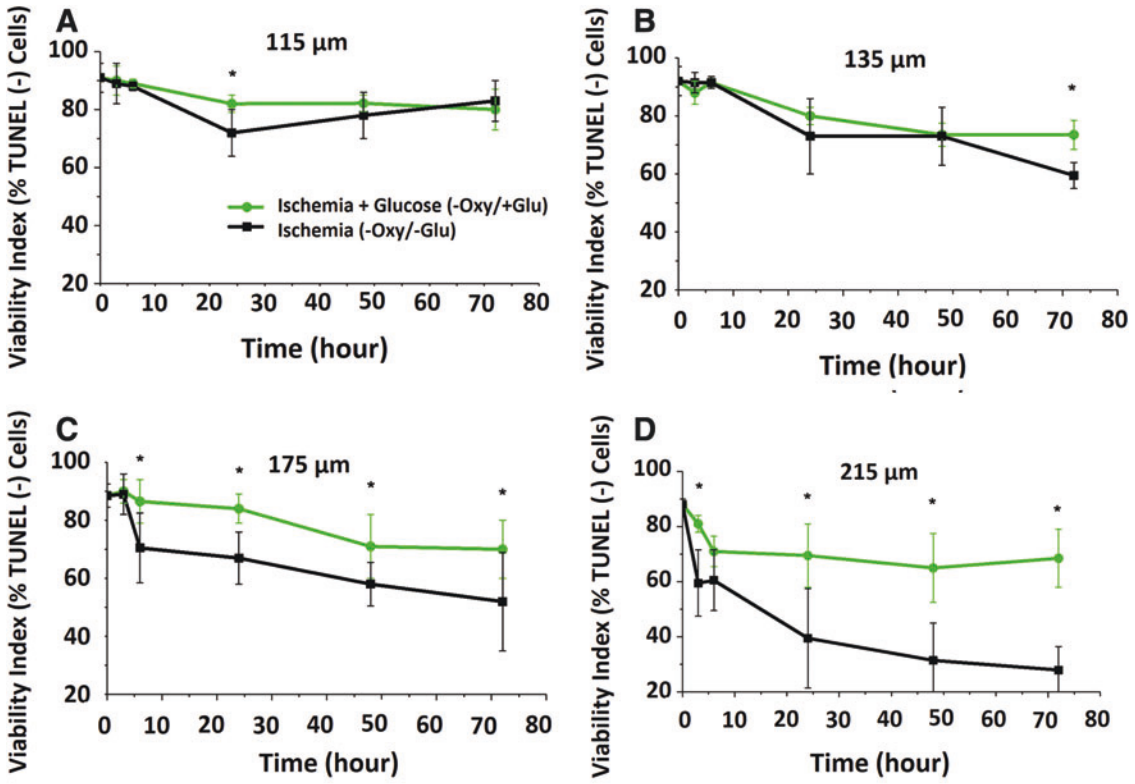

FIG. 7. Increased glucose availability sustains cell viability over time in larger spheroids. **(A–D)** Quantification of cell viability when comparing ischemic (–Oxy/–Glu) and ischemia + glucose (–Oxy/+Glu) culture conditions at 0, 3, 6, 24, 48, and 72 h for **(A)** 115 µm, **(B)** 135 µm, **(C)** 175 µm, and **(D)** 215 µm spheroids. For each culture condition and time point, $n = 8$ spheroids for each spheroid size group and time point. *Significant difference between culture conditions at each time point between spheroid size groups ($p < 0.05$). Color images are available online.

defined in the computational model and previous experimental trials, we conducted a direct longitudinal comparison of ischemic as well as ischemic + glucose (–Oxy/+Glu) conditions at various time points leading up to 72 h (Fig. 7). For the 115 µm spheroid group, there exhibited little difference between the viability indexes of the two conditions for each time point, resulting in high viability for both conditions relative to other groups. For the 135 µm spheroid group, the +Glu group showed greater improvement over the ischemic group at the 72 h time point. However, for both the 175 and 215 µm spheroid groups, the +Glu groups showed improvement almost immediately, with a distinct separation between the viability indexes for the 215 µm culture conditions.

Discussion

hADSCs have emerged as a promising cell source for treating ischemic diseases. Many studies have demonstrated their beneficial properties, including their ability to promote angiogenesis through paracrine effects or offer pericyte support of developing vasculature. However, even with the use of tissue-engineered constructs, low rates of cell survival persist. This requires further study into hADSC spheroid response to the ischemic environment, as well as determination of the governing factors that can lead to cell death under these conditions. To accomplish this, we chose to model the ischemic environment and its effects with hADSC spheroids.

By varying metabolic substrate concentrations and spheroid sizes, our data showed that glucose availability more significantly impacted spheroid viability when compared with oxygen availability, as determined by the modeling results, the DNP-mitigated mitochondrial inhibition and longitudinal supporting studies. From a physiological standpoint, this result may be attributable to the stem cell niche of adipose-derived stem cells, whose environment is naturally hypoxic.[4,29,41] As a result, there is no discernable difference in hADSC spheroid glucose consumption rates when comparing hypoxic (–Oxy/+Glu) to control (+Oxy/+Glu) culture spheroid groups (Fig. 3C–F), suggesting that hADSCs prefer to undergo glycolysis for their metabolic demands even when in the presence of high oxygen levels. This was further supported by the similar rates of lactate production in control (+Oxy/+Glu) and hypoxic (–Oxy/+Glu) cultures, as lactate production is an important byproduct of anaerobic glycolysis. Therefore, as revealed by the positive correlation determined through linear regression, adequate spheroid glucose availability is synonymous with overall spheroid viability; however, oxygen does not possess such a relationship with viability. These results support the notion that oxygen does not play a significant role governing glucose metabolism for hADSC spheroids via metabolic pathways. These results may also explain why the reintroduction of glucose to ischemia yielded similar viability when compared with control for all spheroid sizes, even without reintroducing oxygen. To an extent, this challenges the oxygen paradigm that is often cited as the primary limiting

factor in cell delivery-based tissue regeneration. Since the delivery of highly ATP-dependent cells (e.g., cardiomyocytes) would necessitate reestablishing access to oxygen, it may be advantageous to develop engineering strategies favoring the use of stem cells that can instead satisfy their metabolic needs through anaerobic metabolism.

Results from these current studies showed that glucose improved hADSC spheroid survival in the ischemic environment through anaerobic glycolysis. Its effects on the regenerative functionality of the spheroids necessitate further investigations in the future. This can be accomplished by examining gene and protein expression of hADSC spheroids cultured in an ischemic environment with/without supplemented glucose, as well as assessing the therapeutic efficacy of the spheroids in an animal model. In addition, while the observation period of the described study was limited to 72 h, a longer study eventually may be required, as functional vasculature development *in vivo* can take more than 72 h.[42] Finally, P6 ~ 7 hADSCs were used in the assays to produce a sufficient number of cells to complete all the necessary experiments. Our results verify that passage 6 ~ 7 hADSCs prefer anaerobic culturing conditions, which is consistent with the metabolic function of hADSCs of lower passages.

Conclusion

One of the most pressing challenges in stem cell-based therapies for repairing ischemic injury is low cell retention and survival following transplantation. This issue is primarily due to the hostile environment in ischemic sites due to low concentrations of necessary nutrients. hADSCs have emerged as a robust cell source for treating ischemic injury through their prosurvival signaling, upregulation of angiogenic factors, and their relative durability under ischemic conditions. While hADSC microtissues can enhance cellular survival by helping to avoid anoikis, cell washout, and improving expression of prosurvival factors, their avascular properties reduce nutrient diffusion and availability to the center of the microtissues.

In this work, we combined *in vitro* culture and mathematical modeling to reveal the critical role of glucose to improve hADSC spheroid survival in ischemic conditions. This has been attributed to the intrinsic capacity of hADSCs for anaerobic glycolysis. Due to high aqueous solubility, glucose can be effectively delivered in large quantities with hADSC microtissues to the ischemic injury site *in vivo*. This provides a promising strategy for improving hADSC spheroid survival and retention to an ischemic site posttransplantation. Although the finite element computational model developed in the study specifically examined the effects of nutrient diffusion on avascular spheroid viability, it can be adapted to model more complex scaffold structures (e.g., cell sheets, lattices) or organoid models (i.e., multicellular microtissues). The synergistic application of mathematical modeling and *in vitro* culture model provides a powerful transplantation and establish a solid foundation upon which to create novel strategies for improving cell survival after transplantation.

Acknowledgments

The work is supported by the National Institutes of Health (8P20 GM103444, 1R01HL133308-01A1), the National Science Foundation (NSF-1655740), the NIH Cardiovascular Training Grant (T32 HL007260). This study used the services of the Morphology, Imaging, and Instrumentation Core, which is supported by NIH-NIGMS P30 GM103342 to the South Carolina COBRE for Developmentally Based Cardiovascular Diseases. The work was performed at the Clemson-MUSC Bioengineering Program.

Disclosure Statement

We have no competing financial interests to disclose.

References

1. Cai, L., Johnstone, B.H., Cook, T.G., *et al.* IFATS collection: human adipose tissue-derived stem cells induce angiogenesis and nerve sprouting following myocardial infarction, in conjunction with potent preservation of cardiac function. Stem Cells **27,** 230, 2009.
2. Mizuno, H., Itoi, Y., Kawahara, S., Ogawa, R., Akaishi, S., and Hyakusoku, H. In vivo adipose tissue regeneration by adipose-derived stromal cells isolated from GFP transgenic mice. Cells Tissues Organs **187,** 177, 2008.
3. Izadpanah, R., Trygg, C., Patel, B., *et al.* Biologic properties of mesenchymal stem cells derived from bone marrow and adipose tissue. J Cell Biochem **99,** 1285, 2006.
4. Gimble, J.M., and Nuttall, M.E. Adipose-derived stromal/stem cells (ASC) in regenerative medicine: pharmaceutical applications. Curr Pharm Des **17,** 332, 2011.
5. Rehman, J., Traktuev, D., Li, J., *et al.* Secretion of angiogenic and antiapoptotic factors by human adipose stromal cells. Circulation **109,** 1292, 2004.
6. Mazo, M., Gavira, J.J., Pelacho, B., and Prosper, F. Adipose-derived stem cells for myocardial infarction. J Cardiovasc Transl Res **4,** 145, 2011.
7. Karantalis, V., and Hare, J.M. Use of mesenchymal stem cells for therapy of cardiac disease. Circ Res **116,** 1413, 2015.
8. Faiella, W., and Atoui, R. Therapeutic use of stem cells for cardiovascular disease. Clin Transl Med **5,** 34, 2016.
9. Nakagami, H., Morishita, R., Maeda, K., Kikuchi, Y., Ogihara, T., and Kaneda, Y. Adipose tissue-derived stromal cells as a novel option for regenerative cell therapy. J Atheroscler Thromb **13,** 77, 2006.
10. Zhang, M., Methot, D., Poppa, V., Fujio, Y., Walsh, K., and Murry, C.E. Cardiomyocyte grafting for cardiac repair: graft cell death and anti-death strategies. J Mol Cell Cardiol **33,** 907, 2001.
11. Don, C.W., and Murry, C.E. Improving survival and efficacy of pluripotent stem cell-derived cardiac grafts. J Cell Mol Med **17,** 1355, 2013.
12. Hirt, M.N., Hansen, A., and Eschenhagen, T. Cardiac tissue engineering: state of the art. Circ Res **114,** 354, 2014.
13. Laflamme, M.A., and Murry, C.E. Regenerating the heart. Nat Biotechnol **23,** 845, 2005.
14. Follmar, K.E., Prichard, H.L., DeCroos, F.C., *et al.* Combined bone allograft and adipose-derived stem cell autograft in a rabbit model. Ann Plast Surg **58,** 561, 2007.
15. Vunjak-Novakovic, G., Tandon, N., Godier, A., *et al.* Challenges in cardiac tissue engineering. Tissue Eng Part B Rev **16,** 169, 2010.
16. Davis, B.H., Morimoto, Y., Sample, C., *et al.* Effects of myocardial infarction on the distribution and transport of nutrients and oxygen in porcine myocardium. J Biomech Eng **134,** 101005, 2012.
17. Robey, T.E., Saiget, M.K., Reinecke, H., and Murry, C.E. Systems approaches to preventing transplanted cell death in cardiac repair. J Mol Cell Cardiol **45,** 567, 2008.

18. Tulloch, N.L., Muskheli, V., Razumova, M.V., *et al.* Growth of engineered human myocardium with mechanical loading and vascular coculture. Circ Res **109,** 47, 2011.
19. Fennema, E., Rivron, N., Rouwkema, J., van Blitterswijk, C., and de Boer, J. Spheroid culture as a tool for creating 3D complex tissues. Trends Biotechnol **31,** 108, 2013.
20. Lin, Y.C., Grahovac, T., Oh, S.J., Ieraci, M., Rubin, J.P., and Marra, K.G. Evaluation of a multi-layer adipose-derived stem cell sheet in a full-thickness wound healing model. Acta Biomater **9,** 5243, 2013.
21. Bhang, S.H., Cho, S.W., La, W.G., *et al.* Angiogenesis in ischemic tissue produced by spheroid grafting of human adipose-derived stromal cells. Biomaterials **32,** 2734, 2011.
22. Bolli, R., and Ghafghazi, S. Stem cells: cell therapy for cardiac repair: what is needed to move forward? Nat Rev Cardiol **14,** 257, 2017.
23. Griffith, C.K., Miller, C., Sainson, R.C., *et al.* Diffusion limits of an in vitro thick prevascularized tissue. Tissue Eng **11,** 257, 2005.
24. Weinberger, F., Breckwoldt, K., Pecha, S., *et al.* Cardiac repair in guinea pigs with human engineered heart tissue from induced pluripotent stem cells. Sci Transl Med **8,** 363ra148, 2016.
25. Brown, D.A., MacLellan, W.R., Laks, H., Dunn, J.C., Wu, B.M., and Beygui, R.E. Analysis of oxygen transport in a diffusion-limited model of engineered heart tissue. Biotechnol Bioeng **97,** 962, 2007.
26. Laflamme, M.A., Chen, K.Y., Naumova, A.V., *et al.* Cardiomyocytes derived from human embryonic stem cells in pro-survival factors enhance function of infarcted rat hearts. Nat Biotechnol **25,** 1015, 2007.
27. Kocher, A.A., Schuster, M.D., Szabolcs, M.J., *et al.* Neovascularization of ischemic myocardium by human bone-marrow-derived angioblasts prevents cardiomyocyte apoptosis, reduces remodeling and improves cardiac function. Nat Med **7,** 430, 2001.
28. Fernandes, S., Chong, J.J.H., Paige, S.L., *et al.* Comparison of human embryonic stem cell-derived cardiomyocytes, cardiovascular progenitors, and bone marrow mononuclear cells for cardiac repair. Stem Cell Rep **5,** 753, 2015.
29. Mischen, B.T., Follmar, K.E., Moyer, K.E., *et al.* Metabolic and functional characterization of human adipose-derived stem cells in tissue engineering. Plast Reconstr Surg **122,** 725, 2008.
30. Pattappa, G., Heywood, H.K., de Bruijn, J.D., and Lee, D.A. The metabolism of human mesenchymal stem cells during proliferation and differentiation. J Cell Physiol **226,** 2562, 2011.
31. Brown, D.A., Perry, J.B., Allen, M.E., *et al.* Expert consensus document: mitochondrial function as a therapeutic target in heart failure. Nat Rev Cardiol **14,** 238, 2017.
32. Tan, Y., Richards, D., Xu, R., *et al.* Silicon nanowire-induced maturation of cardiomyocytes derived from human induced pluripotent stem cells. Nano Lett **15,** 2765, 2015.
33. Mylotte, L.A., Duffy, A.M., Murphy, M., *et al.* Metabolic flexibility permits mesenchymal stem cell survival in an ischemic environment. Stem Cells **26,** 1325, 2008.
34. Glicklis, R., Merchuk, J.C., and Cohen, S. Modeling mass transfer in hepatocyte spheroids via cell viability, spheroid size, and hepatocellular functions. Biotechnol Bioeng **86,** 672, 2004.
35. Rumsey, W.L., Schlosser, C., Nuutinen, E.M., Robiolio, M., and Wilson, D.F. Cellular energetics and the oxygen dependence of respiration in cardiac myocytes isolated from adult rat. J Biol Chem **265,** 15392, 1990.
36. Venkatasubramanian, R., Henson, M.A., and Forbes, N.S. Integrating cell-cycle progression, drug penetration and energy metabolism to identify improved cancer therapeutic strategies. J Theor Biol **253,** 98, 2008.
37. Radisic, M., Deen, W., Langer, R., and Vunjak-Novakovic, G. Mathematical model of oxygen distribution in engineered cardiac tissue with parallel channel array perfused with culture medium containing oxygen carriers. Am J Physiol Heart Circ Physiol **288,** H1278, 2005.
38. Rouwkema, J., Rivron, N.C., and van Blitterswijk, C.A. Vascularization in tissue engineering. Trends Biotechnol **26,** 434, 2008.
39. Venkatasubramanian, R., Henson, M.A., and Forbes, N.S. Incorporating energy metabolism into a growth model of multicellular tumor spheroids. J Theor Biol **242,** 440, 2006.
40. Tan, Y., Richards, D., Coyle, R.C., *et al.* Cell number per spheroid and electrical conductivity of nanowires influence the function of silicon nanowired human cardiac spheroids. Acta Biomater **51,** 495, 2017.
41. Gimble, J.M., Katz, A.J., and Bunnell, B.A. Adipose-derived stem cells for regenerative medicine. Circ Res **100,** 1249, 2007.
42. Stevens, K.R., Kreutziger, K.L., Dupras, S.K., *et al.* Physiological function and transplantation of scaffold-free and vascularized human cardiac muscle tissue. Proc Natl Acad Sci U S A **106,** 16568, 2009.

Address correspondence to:
Ying Mei, PhD
Department of Bioengineering
Clemson University
68 President St.
Room BE310
Charleston, SC 29425

E-mail: mei@clemson.edu

Received: June 2, 2018
Accepted: September 17, 2018
Online Publication Date: October 30, 2018